Published in final edited form as:

Brain Res. 2017 September 15; 1671: 1–13. doi:10.1016/j.brainres.2017.06.024.

Functional perturbation of forebrain principal neurons reveals differential effects in novel and well-learned tasks

Emily T. Stoneham, **Daniel G. McHail**, **Katelyn N. Boggs**, **Sarah H. Albani**, **Jason A. Carty**, **Rebekah C. Evans**, **Kelly A. Hamilton**, **Victoria M. Saadat**, **Samanza Hussain**, **Maggie E. Greer**, and **Theodore C. Dumas***

Department of Molecular Neuroscience, George Mason University, Fairfax, VA, USA

Abstract

Neural circuits in mammalian brains consist of large numbers of different cell types having different functional properties. To better understand the separate roles of individual neuron types in specific aspects of spatial learning and memory, we perturbed the function of principal neurons *in vivo* during maze performance or in hippocampal slices during recording of evoked excitatory synaptic potentials. Transgenic mice expressing the Drosophila allatostatin receptor (AlstR) in cortical and hippocampal pyramidal cells were tested on an elevated plus maze, in a Y-maze, and in the Morris water maze. Relative to a control cohort, AlstR-positive mice treated with allatostatin exhibited no difference in open arm dwell time on the elevated plus maze or total number of arm entries in a Y-maze, but displayed reduced spontaneous alternation. When animals received massed or spaced training trials in the Morris water maze, and the peptide was delivered prior to an immediate probe, no effects on performance were observed. When the peptide was delivered during a probe trial performed 24 h after seven days of spaced training, allatostatin delivery to AlstR positive mice enhanced direct navigation to the escape platform. Combined, these results suggest that cortical and hippocampal pyramidal neurons are required during spatial decisionmaking in a novel environment and compete with other neural systems after extended training in a long-term reference memory task. In hippocampal slices collected from AlstR positive animals, allatostatin delivery produced frequency dependent alterations in the Schaffer collateral fiber volley (attenuated accommodation at 100 Hz) and excitatory postsynaptic potential (attenuated facilitation at 5 Hz). Combined, the neural and behavioral discoveries support the involvement of short-term plasticity of Schaffer collateral axons and synapses during exploration of a novel environment and during initial orientation to a goal in a well-learned setting.

Keywords

Allatostatin receptor; GIRK; Hippocampus; Pyramidal neuron; Spatial learning and memory

*Corresponding author at: Department of Psychology, George Mason University, 4400 University Drive, Mail Stop 2A1, Fairfax, VA 22030, USA., tdumas@gmu.edu (T.C. Dumas).

Disclosure

There are no conflicts of interest for any authors of this study.

1. Introduction

Prior work has revealed differential involvement of the hippocampus and striatum in spatial learning and memory tasks that require repetitive training (Dumont and Taube, 2015). In general, the hippocampus is heavily involved early in training, when navigation is controlled more by attentive processing of spatial landmarks, and its contribution declines as performance becomes more procedural and reliant on the striatum (Hicks, 1964; Packard, 1999; Packard and McGaugh, 1996; Packard and White, 1991; Schmitzer-Torbert, 2007). In well-learned dual solution tasks (that can be solved with both spatial and procedural strategies), both the hippocampus and striatum compete for influence over behavior (Lee et al., 2008; Packard et al., 1989) supporting complex regulation of performance that leverages speed and flexibility (Devan et al., 1996; Hamilton et al., 2004). Some plasticity mechanisms that potentially subserve the shift in navigation strategy use with extended training have been identified (Hawes et al., 2015; Yin et al., 2009; Gardner et al., 2016). However, these candidate neural mechanisms reflect population averages and say little about the specific contributions of different types of neurons in both hippocampal and striatal circuits. Greater understanding of how these navigation circuits enable movement to distant goals may be gained by determining how separate components within these circuits individually contribute to information processing and behavioral performance.

Dissection of neural circuits at a cellular level is made possible through genetically encoded neuronal activators and deactivators (Huang and Zeng, 2013). Recent development of ligand and light mediated voltage regulators (Bernstein and Boyden, 2011) and activity-dependent designer receptor systems (Armbruster et al., 2007) has enabled more sophisticated analyses of mammalian neural circuits (Lykken and Kentros, 2014). While referred to as “silencing” systems, these different genetic-based approaches directly alter neuron membrane potential, but do not always completely prevent action potential discharge and have advantages and disadvantages depending on the anatomical target and scientific question. Optogenetic tools provide cell-specific expression and temporal control over membrane potential on the order of milliseconds. While optogenetics are powerful for investigation of the roles of specific neuron types in circuit function and behavior, this approach also requires implantation of a light source into the region of interest and is better suited to small, local networks (Bernstein and Boyden, 2011). Larger circuits may be better targeted with pharmacogenetic approaches that combine cell-specific expression of a unique receptor and systemic or ventricular delivery of its corresponding ligand (Conklin et al., 2008). Along this line, research employing designer receptors exclusively activated by designer drugs (DREADDs, Armbruster et al., 2007) has probed the involvement of forebrain principle neurons in spatial learning (Alexander et al., 2009) and contextual memory consolidation (Zhu et al., 2014) and, when driven by an activity-dependent promoter, has provided insight into the importance of neural ensemble reactivation for memory recall (Garner et al., 2012).

Comparable to DREADDs for large circuit analysis is expression of the Drosophila allatostatin receptor (AlstR) and delivery of the natural ligand, allatostatin (Lechner et al., 2002; Tan et al., 2006). AlstRs are G-protein coupled receptors that link to inward rectifying potassium channels (GIRKs) and reduce neuronal discharge upon binding of allatostatin (Wehr et al., 2009). Thus, AlstRs operate as non-native ligand-gated modifiers of neuronal

function in mammalian tissues (Lechner et al., 2002; Lüscher and Slesinger, 2010; Tan et al., 2006). Cre-dependent expression of AlstRs in excitatory or inhibitory neurons in the forebrain of mice produced opposite effects on population neuronal activation measures but similar impairments in long-term object recognition memory (Haettig et al., 2013), suggesting codependence of this form of memory on excitatory and inhibitory neurons. Wehr et al. (2009) developed a line of transgenic mice that express AlstRs under transcriptional control of the tetracycline response element (Mansuy and Bujard, 2000). Cell type and anatomical region of expression were controlled by crossing this AlstR mouse line with a driver line that expressed the tetracycline transactivator (tTA) in forebrain principal neurons (Jackson Labs, Mayford et al., 1996). Delivery of allatostatin induced functional inhibition in auditory cortex of AlstR-positive animals *in vivo* and in acutely prepared hippocampal slices, though no behavior experiments were performed. Additional work is needed to show that the AlstR system is appropriate for studying large circuit involvement in complex cognitive skills.

In order to better understand how forebrain circuits control spatial navigation, we tested mice expressing AlstR selectively in cortical and hippocampal pyramidal neurons during exploration of a novel maze environment or during memory retrieval after extended training. Additionally, electrically evoked field potentials were recorded in hippocampal slices from AlstR mice treated with allatostatin. We found that AlstR activation in cortical and hippocampal pyramidal neurons reduced spontaneous alternation in a novel Y-maze, while leaving behavior on the elevated plus maze unaffected, and improved the approach trajectory during a long-term memory probe after extended training in the Morris water maze. In hippocampal slices prepared from AlstR positive mice, action potential discharge during high frequency stimulation was spared and synaptic facilitation during a moderate activation rate was reduced by AlstR activation. These results support changes in short-term plasticity of axon discharge and synaptic transmission as candidate mechanisms for behavioral alterations in novel and well-experienced environments and demonstrate the power of AlstR expression for dissection of brain circuits.

2. Materials and methods

2.1. Animal subjects and genotyping

TRE_AlstR and CaMKII_tTA breeders were generously provided by Kentros lab at the University of Oregon (Wehr et al., 2009a). The specific CaMKII_tTA line (line 84, containing the CaMKII minimal promoter, Mayford et al., 1996) was selected because it expresses tTA heavily in hippocampal pyramidal neurons, less so in other cortical pyramidal cells, minimally in granule cells (no expression in most animals), but not interneurons within these regions (Fig. 1A). The AlstR colony was maintained on a 12hr light/-dark cycle in individually-ventilated cages (Animal Care Systems) and allowed food and water ad libitum. At P21 juveniles were weaned, tail clipped, and ear tagged. Genotypes were determined by PCR on genomic DNA from tail biopsies and agarose electrophoresis or determined commercially (Transnetyx). Only double-positive mice (AT) express the AlstR. All other genotypes are controls and referred to inclusively as wild types. The Institutional Animal Care and Use Committee of George Mason University approved the protocols used in the

study (GMU IACUC protocol #0216), and the animals were cared for in accordance with the National Institutes of Health Guidelines for laboratory animal use and care. All experiments were designed to utilize the minimal number of animals required.

2.2. In situ hybridization

Animals were fully anesthetized with Isoflurane (5% vapor) and transcardially perfused with 4% paraformaldehyde. Harvested brains sat overnight in 4% paraformaldehyde (4 °C) and were then transferred to 30% sucrose (4 °C) until each brain descended (48–72 h). Cryopreserved brains were sectioned using a cryostat (30 μm thickness), mounted directly on magnetic microscope slides (Superfrost Plus), and allowed to dry overnight at room temperature. Slides were stored at −80 °C prior to labeling.

Colorimetric whole mount *in situ* hybridization (ISH) was performed on brain tissue sections representative of genotype and condition and selected for quality of specimen prior to reaction per previous research (Albani et al., 2015). Briefly, each reaction was performed on an equal number of sections across variables. Riboprobe template DNA plasmids coding for tTA or AlstR (generous gifts from Dr. Clifford Kentros) were purified by phenol:chloroform extraction or spin column, digested with appropriate restriction enzymes and used for single-stranded riboprobe generation (DIG RNA labeling kit, Roche). Riboprobe was purified (E.Z.N.A, USA or phenol;chloroform extraction, Roche) and stored at −80 °C until use and thawed only once or twice. For each reaction, sections first underwent a two-hour stringency wash in hybridization buffer (H7033 PerfectHyb™ Plus, Sigma Life Science). Riboprobe was mixed into hot (70 °C) hybridization buffer, applied to the tissue sections at 62 °C, and allowed to incubate at 62 °C overnight. Sections were then washed in 50% Formamide/1 X Saline Sodium Citrate (62 °C) and maleic acid buffer with 0.1% Tween 20 (MABT, room temperature) to remove unbound probe and prepare the tissue for antibody labeling, respectively. Sections were incubated overnight at room temperature in an alkaline-phosphatase (AP) conjugated anti-digoxygenin primary antibody (Roche Applied Science). Following washes in MABT and AP Staining Buffer, color was developed through incubation in NBT/BCIP (Roche Applied Science) for four hours at 37 °C. Slides were then washed and dehydrated through sequential dips in increasing ethanol concentration, defatted with xylenes, and coverslipped. Brightfield images were collected at 10X magnification and tiled to capture entire sagittal sections (Neurolucida, MicroBrighfield). Tissue sections were excluded if labeling occurred outside of the forebrain, indicating non-specificity.

2.3. Allatostatin and peptide delivery system

At two to six months of age, animals were anesthetized with a mixture of isoflurane (5% induction, 1.5–2.5% maintenance) and O_2 (1 L/min), positioned in a stereotax, and intracranially cannulated into either their right or left lateral ventricles (randomized) to allow for peptide delivery throughout the brain. A guide cannula (26 gauge, thin-wall, stainless steel) was inserted to a depth of 1.7 mm past the dura mater at ±1.0 mm medial/lateral and −1.0 mm rostral/caudal to bregma. Animals were allowed to recover for two weeks before behavior testing. An injection cannula (30 gauge, stainless steel, passing 0.5 mm beyond the end of the guide cannula) was inserted into the guide to deliver 2 μl of allatostatin (AL, 3 μg/

μl) or vehicle (ACSF; artificial cerebrospinal fluid) to the lateral ventricle. Fluid was administered at a rate of 0.33 μl/min and the injection cannula was left in place for three minutes following injection. AL delivery terminated twenty minutes prior to maze testing. A dose–response curve was not performed because the range of effectiveness for behavioral studies in mice has been established previously (Chierzi et al., 2012; Gosgnach et al., 2006; Haettig et al., 2013; Ikrar et al., 2012; Tan et al., 2006; Wehr et al., 2009b; Zhou et al., 2009) and the concentration at which we delivered allatostatin (roughly 3 μM) falls near the upper end of the range (10 nM–5 μM) with higher doses potentially altering behavior in WT animals (unpublished observations).

2.4. Elevated plus maze

The elevated plus maze (EPM) is an established assay for anxiety in rodents (Handley and Mithani, 1984; Ohl et al., 2001; Walf and Frye, 2007) and used to address potential changes in anxiety that could impact performance in spatial tasks (McHugh et al., 2004). The testing room (3 m × 3 m) was decorated with various spatial cues on two of the four walls. The remaining two walls contained a door or a bench and shelves. The room was illuminated by two multiple intensity incandescent lamps set at medium intensity and positioned at opposite corners. The maze was made of wood, painted black, and sealed with an epoxy coat (Super Glaze, Rust-Oleum Parks). Arm length was 40 cm, arm width was 9 cm, wall height was 15 cm (around two opposing arms only), and the maze stood 70 cm above the floor. A single animal was placed in the center of the maze and allowed to freely explore for 15 min. Total time spent in the open arms, including when the animal occupied the center square, was used to quantify anxiety levels. The maze surface was wiped down with 70% ethanol before the first trial of the day and between trials.

2.5. Y-maze

Spontaneous alternation in a symmetrical Y-maze is a standard assay for hippocampal integrity in rodents (Blair et al., 2013; Douglas and Raphelson, 1966; Dumas, 2004). The Y-maze was made of wood, painted black, and sealed with an epoxy coat. Arm length was 26 cm, arm width was 10 cm, and wall height was 12 cm. The same animals used for EPM exposure were also tested in the Y-maze in the same procedure room. Two weeks passed between EPM and Y-maze testing and animals were exposed to the Y-maze twice with one week between exposures. For each exposure, a single animal was placed in the center of the maze and allowed to freely explore for 15 min. Total number of arm entries and order of arm entries were measured. Alternation rate was calculated as the number of heterogenous triads divided by the number of possible heterogenous triads (total arm entries – 2). The maze surface was wiped down with 70% ethanol before the first trial of the day and between trials.

2.6. Morris water maze

The Morris Water Maze was used to assess spatial memory after extended training in a task designed to minimize procedural performance. The maze was a large circular black plastic pool (1.2 m diameter) filled with water made opaque by non-toxic white paint (Colorations® Simply Washable tempera paint). A white PVC pipe anchored to the pool bottom and a white end cap at the top (covered by a white soft mesh screen) served as the escape platform. The top surface of the platform stood 1 cm below the surface of the water. The MWM was

set up in separate rooms from the dry mazes. For the massed trial training, the room was 3 m × 3m and was decorated on two walls with various paper and plastic shapes, while the other two walls contained a door or an unused stainless steel trim station. For spaced trial training, the room was 3.6 m × 5.25 m with a set of heavy curtains separating the pool from the recording station and a ring of bed sheets hanging from the ceiling surrounding the pool. The sides of the bed sheets facing the pool were decorated with various fabric or painted shapes. The room was lit by dimmed and frost-panel covered fluorescent lamps pointed at the ceiling.

The same animals used for the EPM and the Y-maze exposures were tested with the massed trial training protocol (two weeks following Y-maze exposure). Separate cohorts of animals were tested according to the spaced trial training protocols. Climbing trials were performed for each animal before spatial training, which consisted of placing the animal in the water with its front paws on the edge of the platform. This was repeated until the animal remained on the platform. For massed training, five blocks of three trials were executed with a 15–25 min inter-block interval. For spaced training, four trials (fifteen minute inter-trial interval) were performed daily for seven or eight days. Animals were released from one of four pseudo-randomized, equally spaced locations around the pool (offset from the platform location by 45°) and allowed a maximum of sixty seconds to locate the platform. If the animal did not find the platform in sixty seconds, it was gently led to the platform with the investigator's index finger. Animals remained on the platform for fifteen seconds at the end of each trial. One minute long probe trials, during which the platform was removed from the pool, were performed either on the same day as training trials (IMM) or twenty-four hours later (24-HR).

2.7. Hippocampal slice preparation and recording

Standard procedures were used to prepare hippocampal slices, extract parameters, and analyze data (Dumas, 2012). Dissection and slicing (450 μm, transverse) were performed in ice-chilled, oxygenated (95% O_2, 5% CO_2) artificial cerebrospinal fluid (ACSF in mM: NaCl 124, KCl 2, $MgSO_4$ 2, $CaCl_2$ 2, KH_2PO_4 1.25, $NaHCO_3$ 26, and glucose 10, pH 7.4). Slices were immediately transferred to an interface recording chamber (Harvard Apparatus, Holliston, MA) and perfused with oxygenated ACSF (1.5 ml/min). Slices incubated at room temperature for 1.5–2 h prior to recording. Recordings were performed at room temperature.

The tips of a bipolar platinum-iridium stimulating electrode were placed at the slice surface in the stratum radiatum at the CA2/CA1 border. A glass pipette filled with ACSF (1–8 MΩ tip resistance) was placed approximately 1 mm from the stimulating electrode in the CA1 stratum radiatum. Stimulus pulses (monophasic, 100 μs, 150 μA) were applied at 0.05 Hz and the recording electrode was advanced gently in 20–30 μm steps to maximize the EPSP. Baseline EPSPs were set to 1 mV, which was roughly 25–30% of the maximum EPSP amplitude. For each experiment, 100 pulses were delivered either at 5 or 100 Hz. Signals were amplified (100X) and band-pass filtered between one and 1000 Hz (Axo-Clamp 2B or MultiClamp, Molecular Devices, Sunnyvale, CA) before being digitized at 10 kHz (DigiData 1200 or 1440A Series A/D interface). Experimental protocols were executed using ClampEx (pClamp, Molecular Devices).

The FP amplitude was taken as the voltage value between two cursors, one placed at the response onset and the other at its most negative deflection (Clampfit, pClamp, Molecular Devices). The EPSP slope was calculated within an 0.8 ms window at the initial descending phase of the response. FP and EPSP values were compared by two-way repeated-measures ANOVAs (genotype × stimulation pulse number). All error bars (and ± values in text) are standard error of the mean.

2.8. Statistics

Elevated plus maze and Y-maze results were compared initially by paired t-tests and ANOVAs (2 × 2 design for all data, 1 × 3 design for the three control groups) and followed up with unpaired t-tests after collapsing control groups that showed no difference. MWM probe performance was analyzed off-line using Topscan software (Cleversys, Inc., Reston VA). For each training trial in the water maze, latency to escape and path length were measured, averaged within block for each animal and then averaged across animals for each condition. For each probe trial, the dwell time for each quadrant and the distance between the animal and the escape location sampled at 1 Hz (distance to platform, DtP) were analyzed. The latter procedure, developed by Michaela Gallagher (Gallagher et al., 1993), has been compared to other analyses and deemed superior for detecting group differences in spatial memory ability (Kapadia et al., 2016; Pereira and Burwell, 2015). We applied this measure to the first ten seconds of each probe trial to analyze the initial orientation to the goal location. Additionally, to take into account the final learning level, each DtP value was normalized by the animal's average escape latency for the final training block preceding each IMM probe. Repeated measures ANOVAs were applied to the escape latency curves, DtP curves, and normalized DtP curves (DtP divided by the mean escape latency for the final training block preceding the probe). Tukey's post hoc was applied to specify individual group differences and Greenhouse-Geisser correction for non-sphericity was applied where appropriate. Contingency chi-squared tests (Condition by quadrant) were used for intergroup comparisons of quadrant distributions, and repeated measures ANOVA was used to identify quadrant dwell time differences for the IMM and 24-HR probes. Where there were fewer than three levels in a group, Bonferroni's correction was used. When data could not pass Mauchly's non-sphericity test, the Greenhouse-Geisser correction was applied. Baseline electrophysiology data were initially compared by ANOVA (2 × 2 design for all data, 1 × 3 design for the three control groups) and followed up with unpaired t-tests after collapsing control groups that showed no difference in the initial ANOVA. Whole burst timelines were compared by repeated-measure ANOVA and defined epochs were compared across experimental groups by paired *t*-test.

3. Results

3.1. In situ hybridization (ISH)

Colorimetric ISH is not quantitative for signal intensity per neuron and is semi-quantitative at best for number of neurons per structure. This assay was performed to qualitatively assess the anatomical patterns of expression for tTA and AlstR. Images of sagittal sections hybridized with tTA and AlstR probe were analyzed to determine which forebrain structures did or did not express tTA or AlstRs. tTA expression was consistently observed in principal

neurons throughout the forebrain, though expression in line 84 was less dense in frontal cortex and dorsal striatum than in previous lines (Mayford et al., 1996) (Fig. 1A). The anatomical pattern for AlstR expressionwas also consistent across sections, but was more limited compared to tTA (Fig. 1B). In the hippocampus, tTA expression was seen in all areas, but only sparsely in area CA3. In contrast, AlstR expression was consistently dense in CA1 pyramidal neurons, incompletely in area CA3 (CA3a and CA3b only), and was absent from area CA2, the dentate gyrus, and the subiculum. We also observed tTA expression in pyramidal cells across the neocortex, including the prefrontal cortex, in the amygdala and in medium spiny neurons throughout the striatum. AlstR expression was observed sparsely across the neocortex, ventral striatum and dorsolateral striatum, but was not seen in the amygdala or the dorsomedial striatum (DMS), which has been implicated in attentive spatial navigation (Devan et al., 2011; Hawes et al., 2015).

3.2. Elevated plus maze (EPM)

Animals were tested on the EPM during treatment with allatostatin or vehicle. While not quantified, there were no overt differences in walking, rearing, or grooming behaviors across groups during the holding period between intracranial infusion and maze exposure. Mean open arm time was not different across control conditions (AT-ACSF, wild type-ACSF, wild type-allatostatin) [$F(2, 5) = 1.281$, $p = 0.355$], so these groups were collapsed into a single control group (CON, n = 56) and compared to AT positive mice that received allatostatin (ATD, n = 22). Mean open arm dwell time did not differ between ATD and CON mice [unpaired *t*-test: $t(19) = 0.414$, $p = 0.684$] (Fig. 2A) suggesting no effect of AlstR activation on basic anxiety levels. However, this single measure should be confirmed by additional tests.

3.3. Y-maze

Two weeks following EPM exposure, the same animals were allowed to explore a symmetrical Y-maze. No differences in arm entries [$F(2, 13) = 1.760$, $p = 0.204$] or alternation rate [$F(2, 13) = 0.119$, $p = 0.948$] were seen between control conditions (AT-ACSF, WT-ACSF, WT-AL), so these groups were collapsed into a single control group (CON, n = 17; ATD, n = 6). A two-way ANOVA comparing arm entries scores revealed no difference between CON and ATD [$F(1, 21) = 0.077$, $p = 0.783$]. However, alternation rate for the ATD group was significantly reduced compared to CON animals [$F(1, 21) = 10.879$ $p < 0.005$] (Fig. 2B). Combined with the results from the EPM, these findings support a selective impact of AlstR activation on spatial navigation in a novel environment.

3.4. Morris water maze

3.4.1. Massed training—The same animals exposed to the EPM and Y-maze were tested in the MWM under massed training conditions in a novel testing room. Briefly, animals were trained for 5 blocks (3 trials per block), infused with allatostatin or vehicle, and then tested on an IMM probe after the fifth block. No differences in escape latencies were observed between control conditions during training [$F(2, 37 = 0.264$, $p = 0.769$], so these conditions were combined (CON, n = 40; ATD, n = 14). There was no effect of training block [RM ANOVA $F(4, 208) = 1.005$, $p = 0.403$] or experimental condition [CON versus

ATD, F(1, 52) = 1.786, p = 0.187] on escape latency (Fig. 3A), supporting similar performance levels prior to AlstR activation.

For the IMM probe, there were no differences in swim speeds [F (2, 23) = 0.777, p = 0.472], DtP [F(2, 23) = 0.761, p = 0.479] or normalized DtP (DtP values divided by the mean escape latency for the final training block preceding the probe) across the first 10 s [F(2, 23) = 0.160, p = 0.853], or in platform crossings [F(2, 31) = 1.814, p = 0.180] across the control groups (WT-AL, WT-ACSF, AT-ACSF). Likewise, a repeated measures ANOVA for time spent per quadrant showed no effect of the control conditions [RM ANOVA F(4.840, 147.619) = 1.750, p = 0.129] and a 3 × 4 contingency chi square test also revealed no difference across control groups [(χ^2 (6) = 7.505, p = 0.224]. Therefore, these three groups were collapsed into a single control group (CON).

As expected, given the similar poor performance during training, there was no difference in number of platform crossings between ATD and CON animals during the IMM probe [F(1, 47) = 0.025, p = 0.875) (Fig. 3B). A contingency Chi Square comparing ATD and CON animals was not significant (χ^2 (3) = 3.084, p = 0.387), nor was a repeated measures ANOVA for time spent per quadrant [RM ANOVA F(2.583, 211.833) = 0.760, p = 0.500] (Fig. 3C, D). As well, across the first 10 s of the IMM probe, there was no effect of sample time RM ANOVA F(2.972, 107.006) = 0.595, p = 0.618) or experimental condition on DtP [F(1, 36) = 1.133, p = 0.294] (Fig. 3E). Combined, these data indicate minimal spatial learning in mice when training trials are massed (Commins et al., 2003), and no effects of AlstR activation on immediate probe performance (enhancing or impairing).

3.4.2. Spaced training: Eight training days with IMM probes on Day 5 and Day 8—Separate cohorts of animals were used for each spaced trial MWM experiment. For the first spaced training experiment, 4 trials per day were performed for a total of 8 consecutive days with peptide or vehicle delivery preceding an IMM probe on Day 5 and Day 8. No performance differences in escape latency were observed between control groups [F(2, 16 = 1.615, p = 0.230], so they were collapsed and into a single control group (CON, n = 38; ATD, n = 14). Escape latencies declined significantly across training days 1–5 [RM ANOVA F(4, 200) = 36.145, p < 0.001] and 6–8 [RM ANOVA F(2, 100) = 7.815, p < 0.005], but no differences in escape latency were observed between control conditions across training days 1–5 [F(2, 35 = 1.118, p = 0.338] or 6–8 [F(2, 37) = 1.584, p = 0.219] (Fig. 4A).

For the Day 5 and the Day 8 probes, no differences across control groups were found for swim speed [Day 5: F(2, 35) = 0.769, p = 0.471; Day 8: F(2, 32) = 0.575, p = 0.568], platform crossings [Day 5: F(2, 35) = 1.469, p = 0.244; Day 8: F(2, 32) = 1.423, p = 0.256], time spent per quadrant [Day 5: RM ANOVA F(4.294, 75.141) = 0.500, p = 0.749; Day 8: RM ANOVA F(4.106, 67.744) = 1.339, p = 0.264], quadrant bias [Day 5: χ^2 (6) = 5.834, p = 0.442; Day 8: (χ^2 (6) = 10.595, p = 0.095] and raw [Day 5: RM ANOVA F(7.753, 135.683) = 0.482, p = 0.863; Day 8: RM ANOVA F (8.091, 129.463) = 1.779, p = 0.086] or normalized DtP across the first ten seconds [Day 5: RM ANOVA F(7.774, 136.039) = 0.446, p = 0.887; Day 8: RM ANOVA F(8.077, 129.225) = 1.716, p = 0.100]. Given the lack of differences across five separate analyses, these control subgroups were combined into a single CON group. Neither average swim speed [Day 5: F(1, 50) = 0.054, p = 0.818; Day 8:

F(1, 43) = 0.232 p = 0.632] nor the number of platform crossings were different between ATD and CON [Day 5: CON, n = 38; ATD, n = 14; t(50) = −0.082, p = 0.935]; Day 8: CON, n = 40; ATD, n = 12; t(46) = −0.274, p = 0.785] (Fig. 4B). Likewise, dwell time per quadrant was not different between CON and ATD on either day [Day 5: RM ANOVA F(2.168, 108.387) = 0.901, p = 0.416; Day 8: RM ANOVA F(2.121, 97.554) = 0.525, p = 0.604], with both groups spending more time in the goal quadrant than any other on Day 5 [CON: F(3, 148) = 10.369, p < 0.001, Tukey post hoc p < 0.001; ATD: F(3, 52) = 8.655, p < 0.001, Tukey Post hoc p < 0.001] although only CON spent most of the time in the goal quadrant on Day 8 [CON: F(3, 140) = 27.316, p < 0.001, Tukey post hoc p < 0.001]. A modified ANOVA revealed no difference in goal bias between CON and ATD groups on Day 5 [F(3, 200) = 1.202, p = 0.310] or Day 8 [F(3, 184) = 0.924, p = 0.430]. Both the CON [F (3, 148) = 10.369, p = 0.000] and ATD groups showed a goal bias on Day 5 [F(3, 52) = 8.655, p = 0.000]. Only CON animals showed a goal bias on Day 8 [F(3, 140) = 27.316, p = 0.000] (Fig. 4C, D). Neither DtP, nor normalized DtP were different between CON and ATD animals over the first ten seconds of the probe on Day 5 [DtP: F (3.875, 193.771) = 0.590, p = 0.665; Normalized DtP: F(3.868, 193.387) = 0.583, p = 0.670] or Day 8 [DtP: F(3.829, 164.632) = 0.444, p = 0.768; Normalized DtP: F(3.824, 164.426) = 0.435 p = 0.775] (Fig. 4E, F). Therefore, when the probe trial was delivered on the same day as training trials, there was minimal effect of AlstR activation on performance.

3.4.3. Spaced Training: Seven training days with a 24-HR probe on Day 8—

Spaced training took place over a total of 7 days, with peptide or vehicle delivery preceding a 24HR probe on Day 8. No performance differences in escape latency were observed between control conditions during training [F(2, 16 = 1.615, p = 0.230], so they were collapsed and into a single control group (CON, n = 18; ATD, n = 9). Escape latencies decreased across training days [RM ANOVA F(3.354, 87.208) = 19.749, p < 0.001], but there was no difference between ATD and CON groups (Fig. 5A).

For the Day 8 probe trial, no differences across control groups were found for platform crossings, time spent per quadrant, quadrant bias, and raw or normalized DtP across the first ten seconds. Therefore, these control subgroups were combined into a single CON group. Average swim speed [F(1,43) = 0.232, p = 0.632], he number of platform crossings [t(26) = 0.708, p = 0.485] (Fig. 5B), time spent in the goal quadrant [RM ANOVA, F(1.752, 45.806] = 1.786, p = 0.183) (Fig. 5C), and goal quadrant biases [χ^2 (2) = 0.616, p < 0.735] (Fig. 5D), were not different between ATD and CON groups. Analysis of initial trajectory (first ten seconds of the DtP curves) showed no main effects of sample time [RM ANOVA, F(1.762, 45.806) = 1.786. p = 0.183] or experimental group [F(1, 26) = 0.273, p = 0.606] (Fig. 5E). However, when normalized by the mean escape latency for the final training block, DtP values were reduced for ATD versus the CON animals [F(1,26) = 6.166, p < 0.05] (Fig. 5F). Note that the first data point reflects distance moved from the starting point (which was identical for both groups), showing more direct initial movement to the goal for the ATD animals. These data indicate better spatial memory performance in the ATD animals and support an inhibitory involvement of some forebrain pyramidal cells in spatial orientation toward a goal in well-trained animals, possibly due to competition between the hippocampus and the DMS (Packard et al., 1989; Lee et al., 2008).

3.5. Electrophysiological recording in hippocampal slices from AlstR and control animals

Electrically-evoked field potentials were recorded in the stratum radiatum of area CA1 to examine the impact of AlstR activation on axon discharge and synaptic transmission (Fig. 6A). Stimulation intensity was adjusted to evoke a 2 mV EPSP amplitude and did not differ across groups [CON, 75.7 μA; ATD, 95.2 μA; $t(29) = 0.80$, $p = 0.43$]. Other measures of baseline synaptic transmission, including FP amplitude and EPSP slope, also revealed no group differences [FP amplitude: $t(29) = 0.10$, $p = 0.92$; EPSP slope: $t(29) = 0.94$, $p = 0.35$] (Fig. 6B). The FP amplitude varied across pulse number at 5 Hz (CON, n = 18; ATD, n = 12) [RM ANOVA: $F(1.785, 42.851) = 39.952$, $p < 0.001$] and 100 Hz stimulation (CON, n = 13; ATD, n = 7) [RM ANOVA: $F(1.785, 2352) = 39.852$, $p < 0.001$] (Fig. 6C). There was no effect of genotype on the FP amplitude at 5 Hz. However, at 100 Hz, early in the burst (pulses 2–4), the FP declined more rapidly for CON slices compared to ATD slices [ANOVA: $F(1,54) = 5.911$, $p = 0.018$]. Later in the burst (pulses 7–57), the FP was reduced in ATD compared to CON slices [ANOVA: $F(1918) = 14.177$, $p = 0.0001$]. Similar to the FP amplitude, the EPSP slope varied across pulse number at 5 Hz [$F(1.921, 42.261) = 40.436$, $p < 0.001$] and 100 Hz [RM ANOVA: $F(1.921, 2156) = 40.436$, $p < 0.001$] (Fig. 6D). Facilitation of the EPSP slope (pulse 2–10) was reduced for the ATD group compared to CON animals [ANOVA: $F(1, 190) = 18.352$, $p < 0.001$]. There was no genotype effect on the EPSP slope at 100 Hz (Fig. 6C). (Fig. 6D). Together, these results support frequency-dependent impacts of AlstR activation on action potential discharge and synaptic transmission.

4. Discussion

We have shown that expression and activation of AlstRs in forebrain principal neurons reduced spontaneous alternation in a novel environment and enhanced the initial approach of well-trained animals to an escape platform during a long-term memory test. The observations that 1) there was no effect of AlstR on behavioral activity levels in the Y-maze or swim speed in the MWM, 2) no performance differences on the elevated plus maze and, 3) opposite impacts of AlstR in novel and well-learned spatial environments, support a primary effect in learning and memory circuits and argue against secondary effects in structures regulating sensory processing, motor ability, or anxiety (though this final conclusion is based on a single measure and will require further investigation). Additionally, the lack of an effect during an immediate probe supports an impact restricted to long-term memory. This rationale is matched by the results from *in situ* hybridization showing the highest rate of AlstR transformation of CA1 pyramidal neurons in the hippocampus. However, expression was also notable in area CA3, the neocortex, and ventral striatum, which cannot be dismissed with respect to interpretation of behavioral results.

Spontaneous alternation has been used as an index for hippocampal integrity since the 1970s (Douglas et al., 1973; Dumas, 2004; Blair et al., 2013). The reduction in spontaneous alternation was not surprising given decades of lesion studies showing the negative impact of hippocampal, septal, and entorhinal cortical lesions on spontaneous alternation (Kirkby et al., 1967; Kimble, 1978; Deacon et al., 2002; Krebs and Parent, 2005; Naert et al., 2013) and more contemporary activity marker studies implicating the hippocampus in spatial learning

in novel environments (Guzowski et al., 2001, 2000). Since AlstR was expressed in area CA1 pyramidal cells, only partially in CA3, and not in the dentate gyrus, area CA2, or the subiculum, the current findings support a need for CA1 or proximal CA3 pyramidal neuron activity to execute spontaneous alternation. However, this interpretation is confounded by cortical expression when these AlstR mice are crossed with mice expressing tTA under transcriptional control of the minimal CaMKII promoter. A driver line with greater anatomical specificity should be used in future replication experiments. Given recent studies in which AlstR was expressed either in excitatory or inhibitory neurons and a similar behavioral result was obtained (impaired long-term memory for object lodation, Haettig et al., 2013), one might expect that a reduction in spontaneous alternation might also be observed following AlstR activation in interneurons in area CA3 or area CA1. However, it is also plausible that interneurons are not required for spatial encoding during free exploration, but only when a delay is imposed between arm selections (Rossi et al., 2012) or when the task is goal directed (Pinto and Dan, 2015). Greater behavioral evaluation after manipulation of interneurons is warranted.

The lack of effect of AlstR activation on most measures taken from MWM probe trials highlights the strength of this system in defining the behavioral consequences of cell-specific alterations in activity. Unlike the sledgehammer pharmacological and mechanical inactivation methods of the past that affected all cells and fibers of passage, the current pharmacogenetic system produces more subtle cognitive disturbances and revealed that the forebrain principle neurons that were perturbed were not necessary for navigating to a known goal location when the memory test occurred on the same day as training. The increase in the directness of approach to the MWM escape location during the 24-hour probe during AlstR activation was intriguing. Since this increase was seen only when the memory was tested twenty-four hours after the most recent training block and not on the same day as training, the effect appears specific to long-term memory. However, it is also possible that the selective impact on long-term versus more immediate memory was a function of the number of pyramidal neurons expressing AlstR, with incomplete transformation of CA1 allowing for sufficient normal network activity to support stronger memories. If all CA1 pyramidal cells expressed AlstR, performance in the immediate probe might have also been affected. Human and non-human primate studies reveal a decrementing role for the hippocampus in the retrieval of remotely stored memories (Broadbent et al., 2010; Martin and Clark, 2007; Squire et al., 2001), (Martin and Clark, 2007; Squire et al., 2001) while rodent studies report amnesia that is temporally ungraded (Bolhuis et al., 1994; Mumby et al., 1999; Sutherland et al., 2001). The current results support the idea that the hippocampus plays less of a role in more immediate memory recall after extended training (no AlstR effect on IMM probes) but remains involved in long-term spatial memory retrieval (improved performance in AlstR mice on 24-hour probe), though its contribution appears to negatively impact performance in well-learned spatial reference memory tasks.

In dual-solution spatial and cued learning tasks, during the acquisition phase, hippocampal lesions disrupted spatial learning, but enhanced cued learning (Lee et al., 2008). In the current study, if the hippocampus alone was guiding spatial memory, one might expect a behavioral deficit during AlstR activation. The outcome is a reminder that the hippocampus is part of a larger network guiding the use of spatial context for navigation (Ekstrom et al.,

2014) and suggests that even after extended training in a task designed to minimize procedural navigation learning (random start locations), structures in addition to the hippocampus support goal-directed navigation (Packard et al., 1989; Lee et al., 2008). One primary structure is the DMS, which has been shown to be involved in the learning (Devan et al., 1996; Fouquet et al., 2013; Lee et al., 2014; Hawes et al., 2015) and memory phases of spatial water maze tasks (Lozano et al., 2013). We observed no AlstR expression in the DMS. Since there was no effect of AlstR activation on IMM probe performance and an improvement in the 24-hour probe, it is possible that, after seven days of training, the DMS or another structure outside of the hippocampus (not expressing AlstRs) is able to support memory-based spatial navigation for at least a day after training. Although AlstR expression was observed in multiple forebrain structures and effects in these additional regions cannot be ruled out, the current findings match well with the hippocampus-striatum competition hypothesis.

When applied to hippocampal slices from AlstR-positive animals, allatostatin attenuated the early reduction in the FP amplitude that occurred during high frequency stimulation and reduced synaptic facilitation at moderate stimulation frequency. The observation that later in the 100 Hz burst, the FP decayed more in the ATD animals is less interesting because, rarely if ever *in vivo*, do hippocampal pyramidal neurons discharge at 100 Hz for more than a handful of APs in healthy awake behaving animals (Paulsen and Sejnowski, 2000). One potential mediating mechanism for the effect on the FP would be the ability of AlstR-gated potassium channels to maintain a hyperpolarized membrane potential in the face of an activity level that would normally induce depolarization-dependent inactivation of sodium channels. With respect to the EPSP facilitation at 5 Hz, it may be that GIRK activation after the first stimulus reduces dendritic integration by acting as a frequency-dependent excitation shunt. This band-rejection filter would act to favor synaptic integration at higher or lower frequencies, as partially evidenced by a lack of AlstR effect on baseline synaptic transmission or at 100 Hz. No impact of AlstR activation on baseline synaptic transmission is in agreement with prior reports of effects on action potentials recorded in the auditory cortex *in vivo* where discharge suppression occurred during but not prior to an auditory stimulus (Wehr et al., 2009). Thus, it may be that observed behavioral effects of AlstR activation are a result of alterations to axon function selectively during high frequency activation or synaptic facilitation during more moderate activity levels or both.

These electrophysiology findings also highlight the fact that optogenetic and chemogenetic “silencing” systems do more than eliminate action potentials. In the same mouse line as used in the current study (Wehr et al., 2009), depolarization-induced action potential discharge recorded in hippocampal pyramidal cells in acutely prepared slices was reduced by AlstR activation, but not completely abolished. Likewise, the *in vivo* recordings in neocortex in that study did not show complete silencing in the local network where allatostatin was delivered. One might predict a somewhat different outcome in the current study if the AlstR-transformed neurons were completely silenced. Furthermore, GIRK channels can alter membrane potential separate from action potential discharge (Kim and Johnston, 2015; Barber et al., 2016) and change the shape of the action potential (Isomoto et al., 1997; Stern et al., 2015), which can then secondarily modify synaptic transmission. Our results highlight

the need apply caution when using the term “silencing” and to consider these additional effects when employing genetic-based systems that alter neuronal physiology.

We have shown that the AlstR can be used as an effective method for cell-specific modifications in neuronal physiology during behavior testing and may be more appropriate than optogenetics for larger structures like the hippocampus due to the size of this structure relative to the light penetrance distance limit for optogenetic systems (Luo et al., 2008). While there are fewer reports on AlstR application in the mammalian CNS, AlstR offers many comparable features of the DREADD system in that cell specificity and expression levels can be regulated by the same transcription tools, the same type of potassium channels (GIRK) is exploited, and large circuits can be targeted. AlstR may hold an advantage over DREADDs in that, while a specific ligand/receptor system is introduced by DREADD expression, a native muscarinic receptor, is also substantially impacted by the DREADD ligand clozapine-N-oxide (CNO), introducing a functional confound (Armbruster et al., 2007). Similarly, it was recently shown that CNO is rapidly metabolized into, clozapine and N-desmethylclozapine (NDMC), atypical antipsychotics that act on numerous endogenous neurotransmitter receptors. Finally, when delivered systemically to Rhesus monkeys, CNO was largely restricted from CNS entry at the blood-brain barrier, drawing into question prior reports of DREADD effects on cognitive abilities after systemic CNO delivery (Raper et al., 2017). Moreover, the AlstR system may provide better temporal control over neural activity than DREADDs, in both latency to onset and return to baseline, as explained Alexander and colleagues in their study of DREADD effects on principle neuron physiology in transgenic mice (2009). Our study helps pave the way for future investigations of the neural bases of learning and memory at the cellular level and in more selective brain regions with genetic-based systems that alter neuronal physiology driven by highly anatomically specific transcription drivers.

Acknowledgments

This research was supported by the Office of Naval Research (ONR#000141010198) and the National Institutes of Health (1R15AG045820-01A1). The authors wish to thank Himika Rahman, Nazanin Valibeigi, Hannah Elwell, Chloe Siebach, Annabel Lee Raboy, Stefanie Howell, Arya Loghmani, and Vanya Vojvodic and for their technical assistance.

Abbreviations

ACh	acetylcholine
ACSF	artificial cerebrospinal fluid
AlstR	allatostatin receptor
Amyg	amygdala
ANOVA	analysis of variance
ATD	double-positive mouse receiving drug
BCIP	5-bromo-4-chloro-3′-indolyphosphate

CaMKII	calmodulin activated protein kinase II
CON	combined control groups
DIG	digoxygenin
DMS	dorsomedial striatum
DREADD	designer receptor exclusively activated by designer drug
DtP	distance to platform
EPM	elevated plus maze
EPSP	excitatory postsynaptic potential
FP	fiber potential
GIRK	G-protein linked inward rectifying potassium channel
GMU	George Mason University
IACUC	institutional animal care and use committee
IMM	immediate probe trial
ISH	*in situ* hybridization
MABT	maleic acid buffer with Tween
MWM	Morris water maze
NBT	nitro blue tetrazolium
PCR	polymerase chain reaction
PFC	prefrontal cortex
PVC	polyvinyl chloride
RM	repeated measures
TRE	tetracycline response element
tTA	tetracycline transactivator
24HP	24-hour probe trial

References

Albani SH, Andrawis MM, Abella RJH, Fulghum JT, Vafamand N, Dumas TC. Behavior in the elevated plus maze is differentially affected by testing conditions in rats under and over three weeks of age. Front Behav Neurosci. 2015; 9:31. http://dx.doi.org/10.3389/fnbeh.2015.00031. [PubMed: 25741257]

Armbruster BN, Li X, Pausch MH, Herlitze S, Roth BL. Evolving the lock to fit the key to create a family of G protein-coupled receptors potently activated by an inert ligand. 2007; 104:5163–5168.

Barber DM, Schönberger M, Burgstaller J, Levitz J, Weaver CD, Isacoff EY, Baier H, Trauner D. Optical control of neuronal activity using a light-operated GIRK channel opener (LOGO). Chem Sci. 2016; 7(3):2347–2352. http://dx.doi.org/10.1039/C5SC04084A. [PubMed: 28090283]

Bernstein JG, Boyden ES. Optogenetic tools for analyzing the neural circuits of behavior. Trends Cogn Sci. 2011; 15:592–600. http://dx.doi.org/10.1016/j.tics.2011.10.003. [PubMed: 22055387]

Blair MG, Nguyen NNQ, Albani SH, L'Etoile MM, Andrawis MM, Owen LM, Oliveira RF, Johnson MW, Purvis DL, Sanders EM, Stoneham ET, Xu H, Dumas TC. Developmental changes in structural and functional properties of hippocampal AMPARs parallels the emergence of deliberative spatial navigation in juvenile rats. J Neurosci. 2013; 33:12218–12228. http://dx.doi.org/10.1523/JNEUROSCI.4827-12.2013. [PubMed: 23884930]

Bolhuis JJ, Stewart CA, Forrest EM. Retrograde amnesia and memory reactivation in rats with ibotenate lesions to the hippocampus or subiculum. Q J Exp Psychol B. 1994; 47:129–150. [PubMed: 8052726]

Broadbent NJ, Squire LR, Clark RE. Sustained dorsal hippocampal activity is not obligatory for either the maintenance or retrieval of long-term spatial memory. Hippocampus. 2010; 20:1366–1375. http://dx.doi.org/10.1002/hipo.20722. [PubMed: 19921702]

Chierzi S, Stachniak TJ, Trudel E, Bourque CW, Murai KK. Activity maintains structural plasticity of mossy fiber terminals in the hippocampus. Mol Cell Neurosci. 2012; 50:260–271. http://dx.doi.org/10.1016/j.mcn.2012.05.004. [PubMed: 22579606]

Commins S, Cunningham L, Har D, Walsh D. Massed but not spaced training impairs spatial memory. 2003; 139:215–223.

Conklin BR, Hsiao EC, Claeysen S, Dumuis A, Srinivasan S, Forsayeth JR, Guettier J, Chang WC, Pei Y, Mccarthy KD, Nissenson RA, Wess J, Bockaert J, Roth BL. Engineering GPCR signaling pathways with RASSLs. 2008; 5:673–678. http://dx.doi.org/10.1038/NMETH.1232.

Deacon RMJ, Bannerman DM, Kirby BP, Croucher A, Rawlins JNP. Effects of cytotoxic hippocampal lesions in mice on a cognitive test battery. Behav Brain Res. 2002; 133:57–68. [PubMed: 12048174]

Devan BD, Goad EH, Petri HL. Dissociation of hippocampal and striatal contributions to spatial navigation in the water maze. Neurobiol Learn Mem. 1996; 66:305–323. http://dx.doi.org/10.1006/nlme.1996.0072. [PubMed: 8946424]

Devan BD, Hong NS, Mcdonald RJ. Neurobiology of Learning and Memory Parallel associative processing in the dorsal striatum : segregation of stimulus – response and cognitive control subregions. Neurobiol Learn Mem. 2011; 96:95–120. http://dx.doi.org/10.1016/j.nlm.2011.06.002. [PubMed: 21704718]

Douglas RJ, Peterson JJ, Douglas DP. The ontogeny of a hippocampus-dependent response in two rodent species. Behav Biol. 1973; 8:27–37. http://dx.doi.org/10.1016/S0091-6773(73)80003-3. [PubMed: 4692161]

Douglas RJ, Raphelson aC. Spontaneous alternation and septal lesions. J Comp Physiol Psychol. 1966; 62:320–322. http://dx.doi.org/10.1037/h0023657. [PubMed: 5338926]

Dumas TC. Early eyelid opening enhances spontaneous alternation and accelerates the development of perforant path synaptic strength in the hippocampus of juvenile rats. Dev Psychobiol. 2004; 45:1–9. http://dx.doi.org/10.1002/dev.20011. [PubMed: 15229871]

Dumont JR, Taube JS. The neural correlates of navigation beyond the hippocampus. Prog Brain Res. 2015; 219:83–102. http://dx.doi.org/10.1016/bs.pbr.2015.03.004. [PubMed: 26072235]

Ekstrom AD, Arnold AEGF, Iaria G. A critical review of the allocentric spatial representation and its neural underpinnings: toward a network-based perspective. Front Hum Neurosci. 2014; 8:803. http://dx.doi.org/10.3389/fnhum.2014.00803. [PubMed: 25346679]

Fouquet C, Babayan BM, Watilliaux A, Bontempi B, Tobin C, Rondi-Reig L. Complementary roles of the hippocampus and the dorsomedial striatum during spatial and sequence- based navigation behavior. PLOS. 2013; 1:8. http://dx.doi.org/10.1371/journal.pone.0067232.

Gallagher M, Burwell R, Burchinal M. Severity of Spatial Learning Impairment in Aging : Development of a Learning Index for Performance in the Morris Water Maze. 1993:107.

Gardner RS, Suarez DF, Robinson-Burton NK, Rudnicky CJ, Gulati A, Ascoli GA, Dumas TC. Differential Arc expression in the hippocampus and striatum during the transition from attentive to

automatic navigation on a plus maze. Neurobiol Learn Mem. 2016; 131:36–45. http://dx.doi.org/10.1016/j.nlm.2016.03.008. [PubMed: 26976088]

Garner AR, Rowland DC, Hwang SY, Baumgaertel K, Roth BL, Kentros C, Mayford M. Generation of a Synthetic Memory Trace. 2012:254.

Gosgnach S, Lanuza GM, Butt SJB, Saueressig H, Zhang Y, Velasquez T, Riethmacher D, Callaway EM, Kiehn O, Goulding M. V1 spinal neurons regulate the speed of vertebrate locomotor outputs. Nature. 2006; 440:215–219. http://dx.doi.org/10.1038/nature04545. [PubMed: 16525473]

Guzowski JF, Lyford GL, Stevenson GD, Houston FP, McGaugh JL, Worley PF, Barnes CA. Inhibition of activity-dependent arc protein expression in the rat hippocampus impairs the maintenance of long-term potentiation and the consolidation of long-term memory. J Neurosci. 2000; 20:3993–4001. [PubMed: 10818134]

Guzowski JF, Setlow B, Wagner EK, McGaugh JL. Experience-dependent gene expression in the rat hippocampus after spatial learning: a comparison of the immediate-early genes Arc, c-fos, and zif268. J Neurosci. 2001; 21:5089–5098. [PubMed: 11438584]

Haettig J, Sun Y, Wood MA, Xu X. Cell-type specific inactivation of hippocampal CA1 disrupts location-dependent object recognition in the mouse. Learn Mem. 2013; 20:139–146. http://dx.doi.org/10.1101/lm.027847.112. [PubMed: 23418393]

Hamilton DA, Rosenfelt CS, Whishaw IQ. Sequential control of navigation by locale and taxon cues in the Morris water task. 2004; 154:385–397. http://dx.doi.org/10.1016/j.bbr.2004.03.005.

Handley SL, Mithani S. Effects of alpha-adrenoceptor agonists and antagonists in a maze-exploration model of “fear”-motivated behaviour. Naunyn Schmiedebergs Arch Pharmacol. 1984; 327:1–5. [PubMed: 6149466]

Hawes SL, Evans RC, Unruh BA, Benkert EE, Gillani F, Dumas XC, Blackwell XKT. Multimodal Plasticity in Dorsal Striatum While Learning a Lateralized Navigation Task. 2015; 35:10535–10549. http://dx.doi.org/10.1523/JNEUROSCI.4415-14.2015.

Hicks L. Effects of overtraining on acquisition and reversal of place and response learning. Psychol Rep. 1964; 15:459–462.

Huang ZJ, Zeng H. Genetic Approaches to Neural Circuits in the Mouse. 2013; 36:183–215. http://dx.doi.org/10.1146/annurev-neuro-062012-170307.

Ikrar T, Shi Y, Velasquez T, Goulding M, Xu X. Cell-type specific regulation of cortical excitability through the allatostatin receptor system. Front Neural Circuits. 2012; 6:2. http://dx.doi.org/10.3389/fncir.2012.00002. [PubMed: 22319474]

Isomoto S, Kondo C, Kurachi Y. Inwardly rectifying potassium channels: their molecular heterogeneity and function. Jpn J Physiol. 1997; 47(1):11–39. [PubMed: 9159640]

Kapadia M, Xu J, Sakic B. The water maze paradigm in experimental studies of chronic cognitive disorders: Theory, protocols, analysis, and inference. Neurosci Biobehav Rev. 2016; 68:195–217. http://dx.doi.org/10.1016/j.neubiorev.2016.05.016. [PubMed: 27229758]

Kimble DP. Effects of combined entorhinal cortex-hippocampal lesions on locomotor behavior, spontaneous alternation and spatial maze learning in the rat. Physiol Behav. 1978; 21:177–187. [PubMed: 693644]

Kirkby RJ, Stein DG, Kimble RJ, Kimble DP. Effects of hippocampal lesions and duration of sensory input on spontaneous alternation. J Comp Physiol Psychol. 1967; 64:342–345. [PubMed: 6050582]

Krebs DL, Parent MB. Hippocampal infusions of pyruvate reverse the memory-impairing effects of septal muscimol infusions. Eur J Pharmacol. 2005; 520:91–99. http://dx.doi.org/10.1016/j.ejphar.2005.08.007. [PubMed: 16150437]

Lechner HAE, Lein ES, Callaway EM. A genetic method for selective and quickly reversible silencing of mammalian neurons. J Neurosci. 2002; 22:5287–5290. 20026527. [PubMed: 12097479]

Lee AS, Andre JM, Pittenger C. Lesions of the dorsomedial striatum delay spatial learning and render cue-based navigation inflexible in a water maze task in mice. Front Behav Neurosci. 2014; 8:42. http://dx.doi.org/10.3389/fnbeh.2014.00042. [PubMed: 24592223]

Lee AS, Duman RS, Pittenger C. A double dissociation revealing bidirectional competition between striatum and hippocampus during learning. 2008:1–6.

Lozano YR, Serafin N, Prado-Alcala RA, Roozendaal B, Quirarte GL. Glucocorticoids in the dorsomedial striatum modulate the consolidation of spatial but not procedural memory. Neurobiol Learn Mem. 2013; 101:55–64. http://dx.doi.org/10.1016/j.nlm.2013.01.001. [PubMed: 23313868]

Luo L, Callaway E, Svoboda K. Genetic dissection of neural circuits. Neuron. 2008; 57:634–660. http://dx.doi.org/10.1016/j.neuron.2008.01.002.Genetic. [PubMed: 18341986]

Lüscher C, Slesinger PA. Emerging roles for G protein-gated inwardly rectifying potassium (GIRK) channels in health and disease. Nat Rev Neurosci. 2010; 11:301–315. http://dx.doi.org/10.1038/nrn2834. [PubMed: 20389305]

Lykken C, Kentros CG. Beyond the bolus: transgenic tools for investigating the neurophysiology of learning and memory. Learn Mem. 2014; 21:506–518. http://dx.doi.org/10.1101/lm.036152.114. [PubMed: 25225296]

Mansuy IM, Bujard H. Tetracycline-regulated gene expression in the brain. Curr Opin Neurobiol. 2000; 10:593–596. http://dx.doi.org/10.1016/S0959-4388(00)00127-6. [PubMed: 11084322]

Martin SJ, Clark RE. The rodent hippocampus and spatial memory: from synapses to systems. Cell Mol Life Sci. 2007; 64:401–431. http://dx.doi.org/10.1007/s00018-007-6336-3. [PubMed: 17256090]

Mayford M, Bach ME, Huang YY, Wang L, Hawkins RD, Kandel ER. Control of memory formation through regulated expression of a CaMKII transgene. Science. 1996; 274:1678–1683. http://dx.doi.org/10.1126/science.274.5293.1678. [PubMed: 8939850]

McHugh SB, Deacon RMJ, Rawlins JNP, Bannerman DM. Amygdala and ventral hippocampus contribute differentially to mechanisms of fear and anxiety. Behav Neurosci. 2004; 118:63–78. http://dx.doi.org/10.1037/0735-7044.118.1.63. [PubMed: 14979783]

Mumby DG, Astur RS, Weisend MP, Sutherland RJ. Retrograde amnesia and selective damage to the hippocampal formation: memory for places and object discriminations. Behav Brain Res. 1999; 106:97–107. [PubMed: 10595425]

Naert A, Gantois I, Laeremans A, Vreysen S, Bergh G, Van Den Arckens L, Callaerts-vegh Z, Hooge RD. Behavioural alterations relevant to developmental brain disorders in mice with neonatally induced ventral hippocampal lesions. Brain Res Bull. 2013; 94:71–81. http://dx.doi.org/10.1016/j.brainresbull.2013.01.008. [PubMed: 23357176]

Ohl F, Toschi N, Wigger A, Henniger MSH, Landgraf R. Dimensions of emotionality in a rat model of innate anxiety. 2001; 115:429–436. http://dx.doi.org/10.1037//0735-7044.115.2.429.

Packard MG. Glutamate infused posttraining into the hippocampus or caudate-putamen differentially strengthens place and response learning. 1999; 96:12881–12886.

Packard MG, Hirsh R, White NM. Differential effects of fornix and caudate nucleus lesions on two radial maze tasks: evidence for multiple memory systems. J Neurosci. 1989; 9:1465–1472. [PubMed: 2723738]

Packard MG, McGaugh JL. Inactivation of hippocampus or caudate nucleus with lidocaine differentially affects expression of place and response learning. Neurobiol Learn Mem. 1996; 65:65–72. [PubMed: 8673408]

Packard MG, White NM. Dissociation of hippocampus and caudate nucleus memory systems by posttraining intracerebral injection of dopamine agonists. Behav Neurosci. 1991; 105:295–306. [PubMed: 1675062]

Paulsen O, Sejnowski TJ. Natural patterns of activity and long-term synaptic plasticity. Curr Opin Neurobiol. 2000; 10:172–180. [PubMed: 10753798]

Pereira T, Burwell R. Using the spatial learning index to evaluate performance on the water maze. Behav Neurosci. 2015; 129:533–539. http://dx.doi.org/10.1037/bne0000078.Using. [PubMed: 26214218]

Pinto L, Dan Y. Cell-type-specific activity in prefrontal cortex during goal-directed behavior. Neuron. 2015; 87:437–450. http://dx.doi.org/10.1016/j.neuron.2015.06.021. [PubMed: 26143660]

Raper, J., Morrison, RD., Daniels, JS., Howell, L., Bachevalier, J., Wichmann, T., Galvan, A. Metabolism and Distribution of Clozapine-N-oxide: Implications for Nonhuman Primate Chemogenetics. ACS Chem Neurosci. 2017. acschemneuro.7b00079. http://dx.doi.org/10.1021/acschemneuro.7b00079

Rossi MA, Hayrapetyan VY, Maimon B, Mak K, Je HS, Yin HH. Prefrontal cortical mechanisms underlying delayed alternation in mice. J Neurophysiol. 2012; 108:1211–1222. http://dx.doi.org/10.1152/jn.01060.2011. [PubMed: 22539827]

Schmitzer-Torbert N. Place and response learning in human virtual navigation : behavioral measures and gender differences. Behav Neurosci. 2007; 121:277–290. http://dx.doi.org/10.1037/0735-7044.121.2.277. [PubMed: 17469917]

Squire LR, Clark RE, Knowlton BJ. Retrograde amnesia. Hippocampus. 2001; 11:50–55. http://dx.doi.org/10.1002/1098-1063(2001)11:1<50::AID-HIPO1019>3.0.CO;2-G. [PubMed: 11261772]

Stern S, Segal M, Moses E. Involvement of potassium and cation channels in hippocampal abnormalities of embryonic Ts65Dn and Tc1 trisomic mice. EBioMedicine. 2015; 2(9):1048–1062. http://dx.doi.org/10.1016/j.ebiom.2015.07.038. [PubMed: 26501103]

Sutherland RJ, Weisend MP, Mumby D, Astur RS, Hanlon FM, Koerner A, Thomas MJ, Wu Y, Moses SN, Cole C, Hamilton DA, Hoesing JM. Retrograde amnesia after hippocampal damage: recent vs. remote memories in two tasks. Hippocampus. 2001; 11:27–42. http://dx.doi.org/10.1002/1098-1063(2001)11:1<27::AID-HIPO1017>3.0.CO;2-4. [PubMed: 11261770]

Tan EM, Yamaguchi Y, Horwitz GD, Gosgnach S, Lein ES, Goulding M, Albright TD, Callaway EM. Selective and quickly reversible inactivation of mammalian neurons in vivo using the drosophila allatostatin receptor. Neuron. 2006; 51:157–170. http://dx.doi.org/10.1016/j.neuron.2006.06.018. [PubMed: 16846851]

Walf, AA., Frye, CA. The use of the elevated plus maze as an assay of anxiety-related behavior in rodents. 2007. http://dx.doi.org/10.1038/nprot.2007.44

Wehr M, Hostick U, Kyweriga M, Tan A, Weible AP, Wu H, Wu W, Callaway EM, Kentros C. Transgenic silencing of neurons in the mammalian brain by expression of the allatostatin receptor (AlstR). J Neurophysiol. 2009a; 102:2554–2562. [Erratum appears in J Neurophysiol 2009 Dec; 102(6):3781]. http://dx.doi.org/10.1152/jn.00480.2009. [PubMed: 19692509]

Wehr M, Hostick U, Kyweriga M, Tan A, Weible AP, Wu H, Wu W, Callaway EM, Kentros C. Transgenic silencing of neurons in the mammalian brain by expression of the allatostatin receptor (AlstR). J Neurophysiol. 2009b; 102:2554–2562. http://dx.doi.org/10.1152/jn.00480.2009. [PubMed: 19692509]

Yin HH, Mulcare SP, Hilario MR, Clouse E, Holloway T, Davis MI, Hansson AC, Lovinger D, Costa RM. Dynamic reorganization of striatal circuits during the acquisition and consolidation of a skill. Nat Neurosci. 2009; 12:333–341. http://dx.doi.org/10.1038/nn.2261. [PubMed: 19198605]

Zhou Y, Won J, Karlsson MG, Zhou M, Rogerson T, Balaji J, Neve R, Poirazi P, Silva AJ. CREB regulates excitability and the allocation of memory to subsets of neurons in the amygdala. Nat Neurosci. 2009; 12:1438–1443. http://dx.doi.org/10.1038/nn.2405. [PubMed: 19783993]

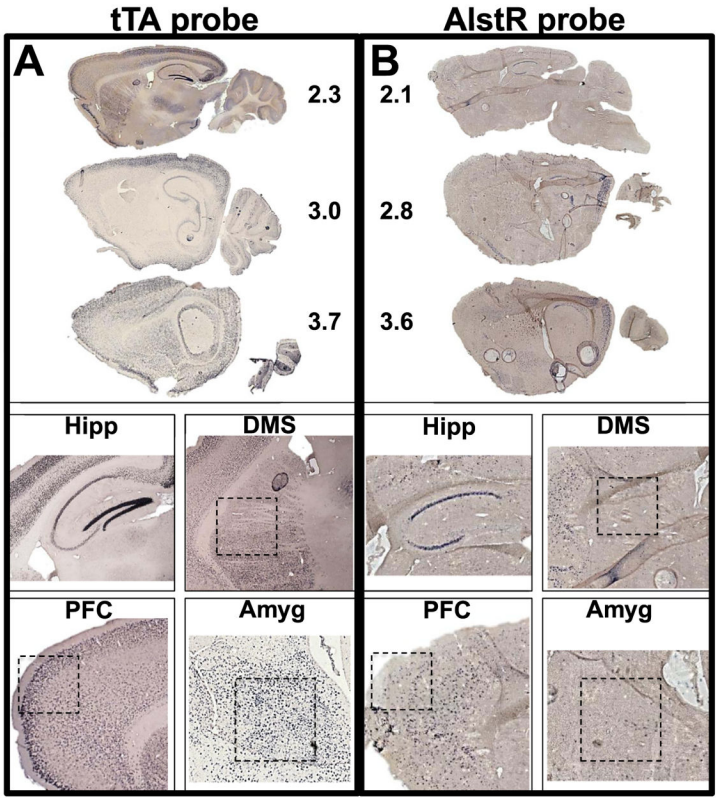

Fig. 1.

Images of colorimetric ISH for tTA and AlstR. A) Complete sagittal images and selected regions from +/+ AlstR mouse brain sections reacted with a tTA probe. B) Complete sagittal images and selected regions from +/+ AlstR mouse brain sections reacted with an AlstR probe. Numbers in top panels indicate distance from midline in mm. Hipp, hippocampus; DMS, dorsomedial striatum; PFC prefrontal cortex; Amyg, amygdala. All images were collected at 10X magnification and tiled (Neurolucida, MBF Bioscience) where necessary.

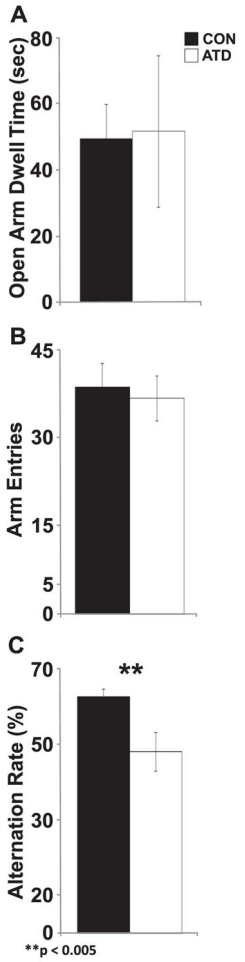

Fig. 2.

Open arm dwell time in the EPM was not affected but spontaneous alternation in a symmetrical Y maze was reduced during silencing of forebrain pyramidal neurons. A) ATD (+/+ receiving allatostatin) and CON animals (all control groups collapsed) spent similar amounts of time in the open arms of the EPM (CON, n = 56; ATD, n = 22). B) Total number of arm entries did not differ across experimental groups (CON, n = 17; ATD, n = 6). C) Alternation rate in the Y maze was reduced in ATD animals compared to CON animals. $^{**}p < 0.005$.

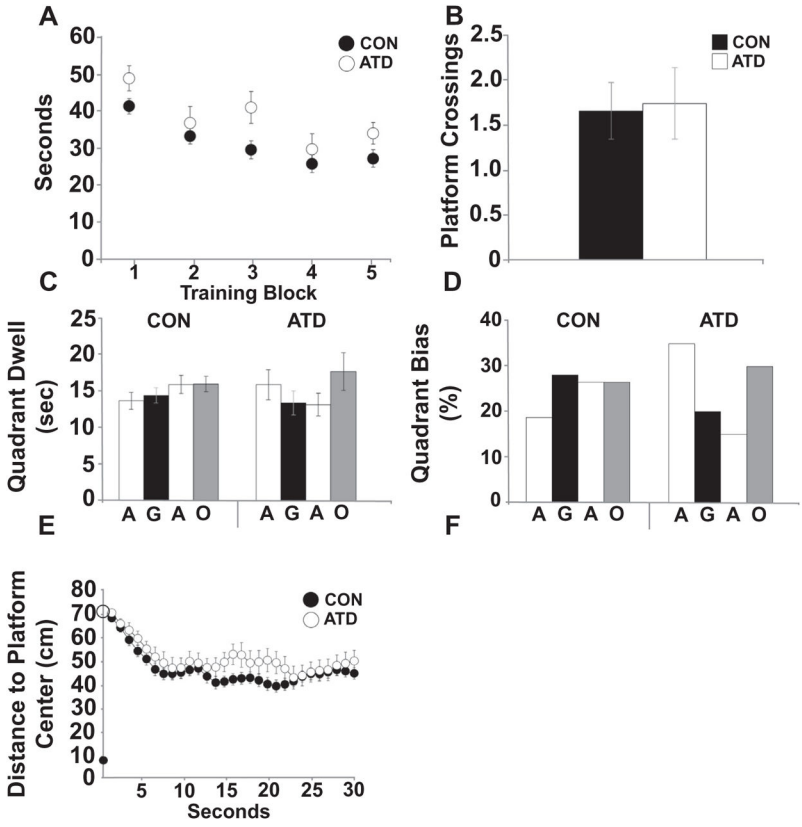

Fig. 3.

Silencing of forebrain pyramidal neurons did not affect spatial learning during massed training. A) Escape latencies during training did not differ between CON and ATD animals (CON, n = 40; ATD, n = 14). B) Number of platform crossings during the IMM probe did not differ between CON and ATD animals; C) Plot of quadrant dwell times during the IMM probe shows that neither CON nor ATD animals spent more time in any given quadrant. G = goal, O = opposite, A = adjacent. D) Plot of quadrant biases (percentage of animals spending most of their time in a given quadrant) during the IMM probe shows that neither CON nor ATD animals exhibited a quadrant bias. E) DtP measured across 10 or 30 s of the IMM probe did not differ between CON and ATD animals. The black circle on the Y-axis indicates the platform edge. The open circle marks starting location for all animals (710 mm).

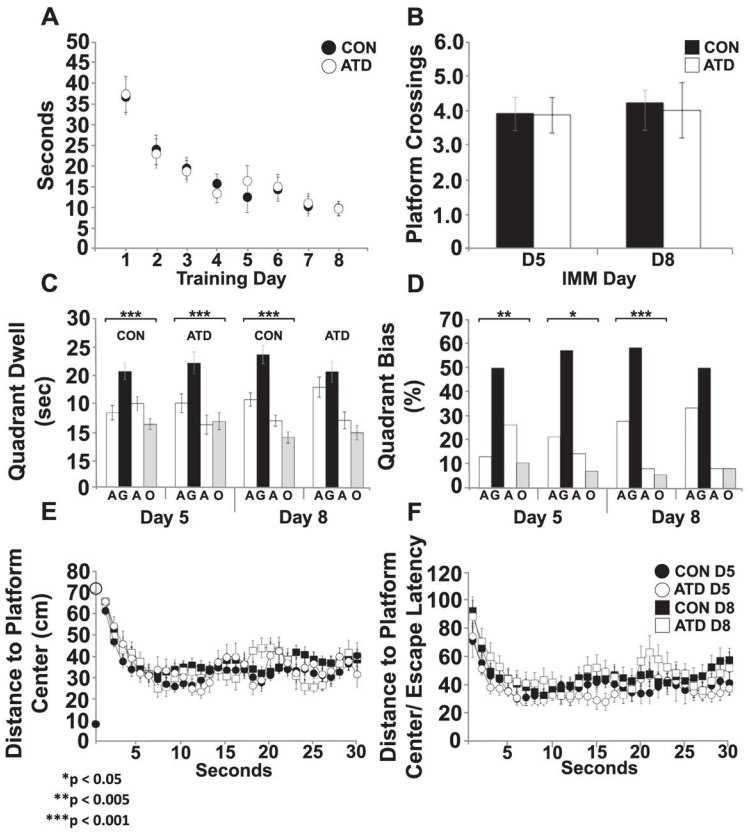

Fig. 4.

Silencing of forebrain pyramidal neurons did not affect spatial learning during 8 days of spaced training. A) Escape latencies during training did not differ between CON and ATD animals on Day 5 (CON, n = 38; ATD, n = 14), or Day 8 (CON, n = 40; ATD, n = 12). B) Number of platform crossings during the IMM probe did not differ between CON and ATD animals for Day 5 or Day 8. C) ATD and CON animals in the amount of time animals spent in each quadrant during the IMM probe on Day 5 or Day 8. Both groups spent more time in the goal quadrant than any other quadrant (Chi Square tests); $^{*}p < 0.05$, $^{**}p < 0.005$, $^{***}p < 0.001$. However, only CON animals spent more time in the goal quadrant than any other on Day 8; $^{***}p < 0.001$. D) Both CON and ATD animals showed a bias for the goal quadrant during the IMM probe on Day 5 (CON, n = 38; ATD, n = 14), but only CON showed a preference on Day 8 (CON, n = 37; ATD, n = 11) $^{*}p < 0.05$, $^{**}p < 0.005$. E) DtP measured across 10 s of the IMM probe on Day 5 or Day 8 did not differ between CON and ATD animals. The black circle on the Y-axis indicates the platform edge. The open circle marks starting location for all animals (710 mm). F) There was no difference between CON and ATD animals for DtP on the IMM probe on either Day 5 or Day 8.

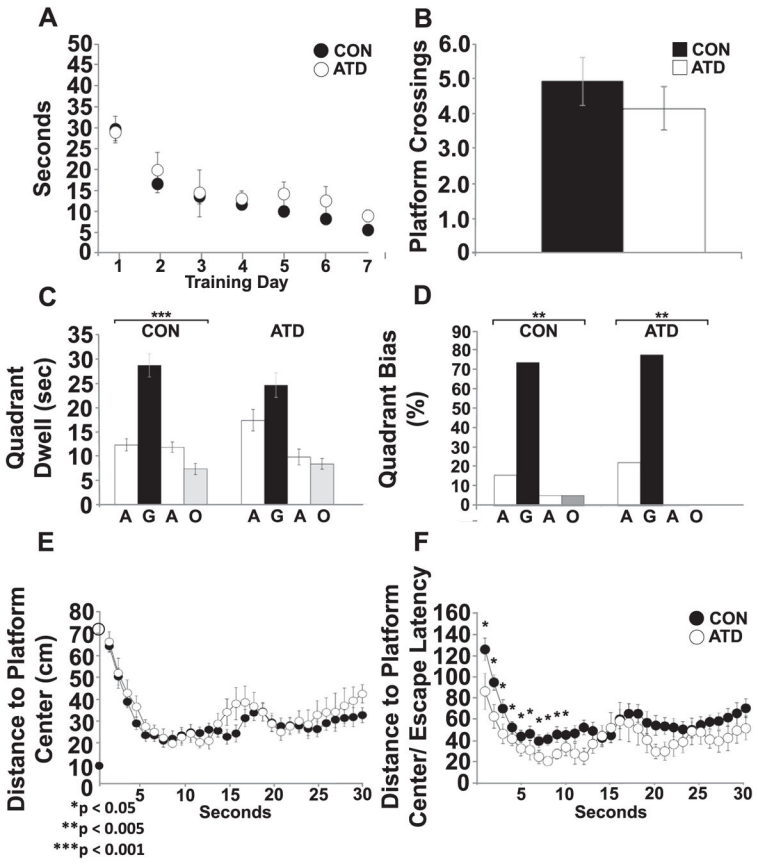

Fig. 5.

Silencing of forebrain pyramidal neurons improved the initial orientation to the goal location during a 24-HR probe. A) Escape latencies during training did not differ between CON and ATD animals (CON, n = 18; ATD, n = 9). B) Number of platform crossings during the 24-HR probe did not differ between CON and ATD animals during the 24HP probe. C) Both CON and ATD animals showed a preference for the goal quadrant during the 24HP$^{**}p < 0.005$ E) DtP measured across 10 s of the 24HP did not differ between CON and ATD animals. The black circle on the Y-axis indicates the platform edge. The open circle marks starting location for all animals (710 mm). F) The first 10 s of the normalized DtP 24HP was reduced for the ATD animals compared to the CON animals [$F(1,26) = 6.166$, $p < 0.05$]; * = $p < 0.05$.

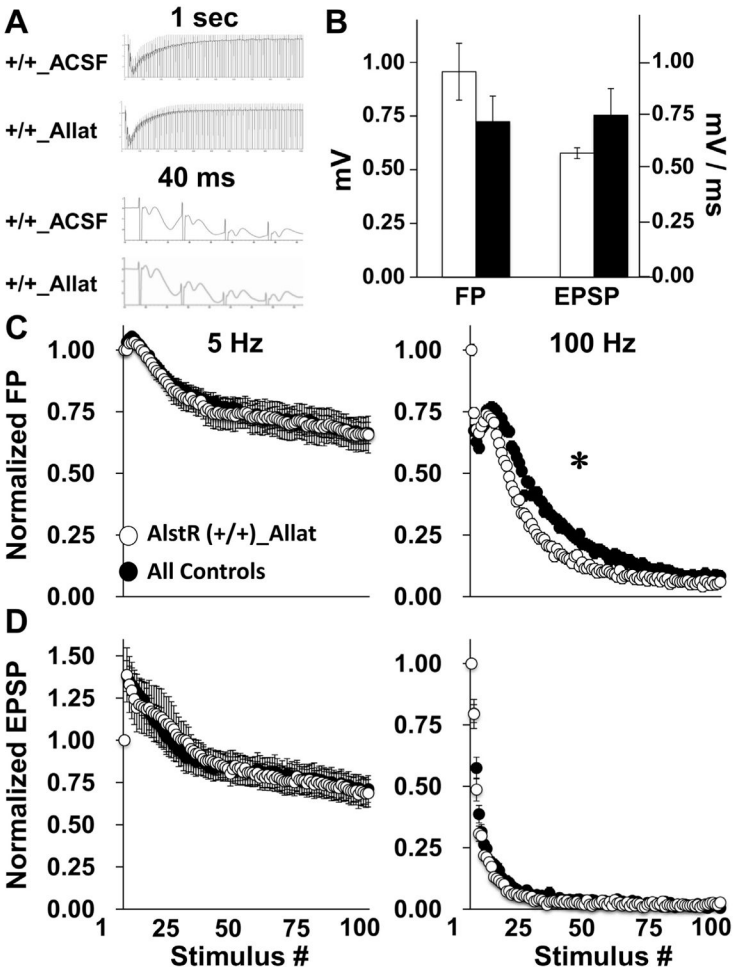

Fig. 6.

AlstR activation in hippocampal slices did not alter baseline synaptic transmission but attenuated synaptic facilitation at 5 Hz and AP accommodation at 100 Hz stimulation. One hundred stimulus pulses were applied at 5 (CON, n = 18; ATD, n = 8) or 100 Hz (CON, n = 13; ATD, n = 7). A) Waveforms show all responses across a 100 Hz burst (top, 1 s) or only the first four responses (bottom, 40 ms) for ATD and CON animals. B) Analyses of responses to the first stimulus pulse for all 5 and 100 Hz burst experiments revealed no difference in the mean FP amplitude or mV EPSP slope (CON, n = 18; ATD, n = 12). C) Mean FP amplitude plotted against stimulus number did not differ between groups at 5 Hz stimulation. At 100 Hz, the FP amplitude decreased more during early stimulus pulses (pulse 2–4) for CON slices compared to ATD slices, but decreased more later in the burst (pulses 7–57) for ATD compared to CON slices. * = $p < 0.05$; *** = $p < 0.0001$. D) Mean EPSP slope plotted against stimulus number did not differ between groups at 100 Hz stimulation. Synaptic facilitation was reduced in ATD compared to CON animals at 5 Hz. ** = $p < 0.001$.